

---

# Effect of spatial variation characteristics on contouring of design storm depth

Ke-Sheng Cheng,<sup>1\*</sup> Chiang Wei,<sup>1</sup> Yen-Ben Cheng<sup>1</sup> and Hui-Chung Yeh<sup>2</sup>

<sup>1</sup> Department of Bioenvironmental Systems Engineering, National Taiwan University, Taipei, Taiwan, ROC

<sup>2</sup> Digital Earth Research Center, Chinese Culture University, Taipei, Taiwan, ROC

---

## Abstract:

The ordinary kriging method, a geostatistical interpolation technique, was applied for developing contour maps of design storm depth in northern Taiwan using intensity–duration–frequency (IDF) data. Results of variogram modelling on design storm depths indicate that the design storms can be categorized into two distinct storm types: (i) storms of short duration and high spatial variation and (ii) storms of long duration and less spatial variation. For storms of the first category, the influence range of rainfall depth decreases when the recurrence interval increases, owing to the increasing degree of their spatial independence. However, for storms of the second category, the influence range of rainfall depth does not change significantly and has an average of approximately 72 km. For very extreme events, such as events of short duration and long recurrence interval, we do not recommend usage of the established design storm contours, because most of the interstation distances exceed the influence ranges. Our study concludes that the influence range of the design storm depth is dependent on the design duration and recurrence interval and is a key factor in developing design storm contours. Copyright © 2003 John Wiley & Sons, Ltd.

KEY WORDS design storm; intensity-duration-frequency curves; kriging; variogram; stormwater management

## INTRODUCTION

The design storm, a crucial element in urban drainage design and hydrological modelling, is a hypothetical storm of specific *storm duration*,  $tr$ , and *recurrence interval*,  $T$ . The total rainfall depth and its time distribution, i.e. the *hyetograph*, are two elements characterizing a design storm. The total rainfall depth of a design storm is usually estimated by hydrological frequency analysis using historic rainfall records. For areas without historic rainfall records, design storm depths are often estimated using design storm data from adjacent sites. For this purpose, a rainfall frequency atlas, i.e. contour maps of design storm depths, has been developed for Florida (Rao, 1991) and the USA (Hershfield, 1961). In Taiwan, although design storm depths are available at many rain-gauge sites, a rainfall frequency atlas has yet to be developed.

During the past two decades there has been a dramatic increase in the development of residential communities in hillslope areas in Taiwan. Authoritative agencies require a stormwater water management plan to be submitted as part of the permit application. Many developments have taken place in areas without rainfall records, and therefore the design storm depth for the project is interpolated using design storm depths available at surrounding sites. Methods of spatial rainfall interpolation include the station-year method, normal-ratio method, arithmetic-mean method, reciprocal-distance-squared method, and isohyetal method (Viessman *et al.*, 1989). The usefulness of each method depends on its interpolation algorithm and complexity of the spatial variation of the rainfall field under investigation. The spatial variability of the rainfall depth varies with the associated time-scale. For example, annual rainfall and monthly rainfall exhibit less spatial variation than

---

\* Correspondence to: Ke-Sheng Cheng, Department of Bioenvironmental Systems Engineering, National Taiwan University, Taipei, Taiwan, ROC. E-mail: rslab@ccms.ntu.edu.tw.

hourly rainfall. Therefore, the arithmetic-mean method may yield a satisfactory result for spatial interpolation of annual rainfall, whereas spatial interpolation of hourly rainfall may require more sophisticated algorithms. In this study we consider the spatial distribution of design storm depth as a random field. In addition, the spatial variation structure of the design storm depth may vary with the duration and recurrence interval of the design storm; therefore, interpolation of design storm depth requires an algorithm that takes into account the spatial variation structure.

Since the early 1970s the kriging method, a geostatistical interpolation technique, has been widely applied to various hydrological research topics, including monitoring network evaluation (Hughes and Lettenmaier, 1981) and spatial estimation of rainfall field and soil properties (Bastin *et al.*, 1984; Chang *et al.*, 1999). Success of the kriging method stems from its capability of modelling the spatial variation structure of a random field. Thus, the objectives of this study are to develop contour maps of design storm depth using the kriging method and to investigate the effect of spatial variation characteristics on construction of design storm contours.

### THEORY OF ORDINARY KRIGING

Kriging is a group of spatial interpolation/estimation methods that takes into account the spatial variation structure of a random field. Major forms of kriging estimation include simple kriging, ordinary kriging, universal kriging, disjunctive kriging, probabilistic kriging, indicator kriging, and co-kriging. These algorithms vary in their assumptions for statistical properties of the random fields. In this study we apply ordinary kriging to interpolation of design storm depths, and therefore only the theory of ordinary kriging is briefly described below.

Let  $Z(x)$  be a random variable defined at location  $x$  and  $\{Z(x), x \in \Omega\}$  be a second-order stationary random field in a spatial domain  $\Omega$ , i.e.

$$E[Z(x)] = \mu_Z \quad \forall x \in \Omega \quad (1)$$

$$\text{Var}[Z(x)] = \sigma_Z^2 \quad \forall x \in \Omega \quad (2)$$

$$\text{Cov}[Z(x_i), Z(x_j)] = \text{Cov}(|x_i - x_j|) = C(|x_i - x_j|) \quad \forall x_i, x_j \in \Omega \quad (3)$$

Under the second-order stationarity assumption, the spatial variation structure of  $\{Z(x)\}$  is independent of spatial locations and is characterized by a *semi-variogram* defined as

$$\gamma(|x_i - x_j|) = \frac{1}{2} \text{Var}[Z(x_i) - Z(x_j)] = \frac{1}{2} E[Z(x_i) - Z(x_j)]^2 \quad (4)$$

The semi-variogram, hereinafter referred to as the *variogram*, and the covariance function are related by

$$\gamma(h) = C(0) - C(h) \quad (5)$$

where  $C(h)$  represents the covariance function of  $Z(x)$  and  $Z(x+h)$ . Figure 1 illustrates the typical variogram of a second-order stationary random field. A variogram has three important parameters: *influence range*, *sill* and the *nugget*. The influence range is the minimum distance  $|x_i - x_j|$  beyond which the two random variables  $Z(x_i)$  and  $Z(x_j)$  become independent. The sill is the asymptotic value of the variogram. For a second-order stationary random field, the sill is numerically the same as the variance of the random variable. Theoretically, the variogram should pass through the origin, however, owing to measurement errors or variation of  $Z(x)$  at a very small spatial scale, an abrupt jump of the variogram near the origin may present. This is called the nugget effect, and the departure of  $\gamma(h)$  from the origin is the nugget value. If the influence range approaches zero, all random variables within the spatial domain  $\Omega$  become independent, and  $\{Z(x), x \in \Omega\}$  is a white noise random field. The variogram of a white noise random field exhibits the pure nugget effect (see Figure 2). A

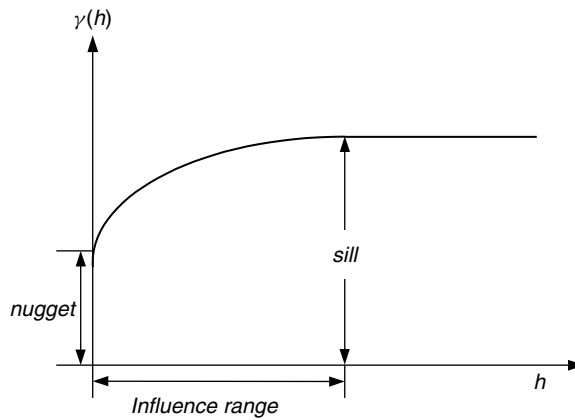


Figure 1. Typical form of a semi-variogram

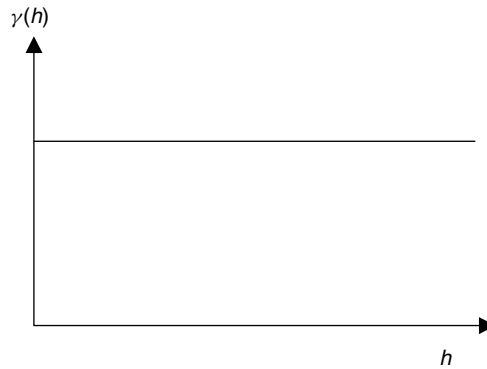


Figure 2. Semi-variogram with pure nugget effect

variogram is conditionally negative definite (Wackernagel, 1995), i.e. under the condition that  $\sum_{i=1}^n \lambda_i = 0$ , it gives

$$-\sum_{i=1}^n \sum_{j=1}^n \lambda_i \lambda_j \gamma_{ij} \geq 0 \quad \forall \lambda_i, \lambda_j \in R \tag{6}$$

where  $\gamma_{ij} = \gamma(|x_i - x_j|)$ .

We now attempt to estimate an unknown value of  $Z$  at  $x_0$ , i.e.  $z(x_0)$ , using observed values  $z(x_i)$ ,  $i = 1, 2, \dots, m$ , at neighbouring locations and the following linear equation

$$\hat{z}(x_0) = \sum_{i=1}^m \lambda_i z(x_i) \tag{7}$$

where  $\lambda_i$  represents weights assigned to measurements  $z(x_i)$ . The ordinary kriging estimator is, by design, a *best linear unbiased estimator* (BLUE) that satisfies the following conditions

$$E[\hat{Z}(x_0)] = E[Z(x_0)] \tag{8}$$

$$\text{minimizing } \text{Var}[\hat{Z}(x_0) - Z(x_0)] \tag{9}$$

The unbiasedness condition of Equation (8) is warranted with unit-sum weights

$$\sum_{i=1}^m \lambda_i = 1 \quad (10)$$

Minimization of the variance of estimation error, under the constraint on weights  $\lambda_i$ , is achieved by introducing a Lagrange multiplier  $\mu$  and minimizing the following term

$$M = \text{Var}[\hat{Z}(x_0) - Z(x_0)] - 2\mu \left( \sum_{i=1}^m \lambda_i - 1 \right) \quad (11)$$

with respect to  $\lambda_i$  and  $\mu$ . Differentiating  $M$  with respect to  $\lambda_i$  and  $\mu$  yields the ordinary kriging system (Journal and Huijbregts, 1978)

$$\begin{bmatrix} \gamma_{11} & \cdots & \gamma_{1i} & \cdots & \gamma_{1m} & 1 \\ \vdots & \ddots & \vdots & \ddots & \vdots & \vdots \\ \gamma_{i1} & \cdots & \gamma_{ii} & \cdots & \gamma_{im} & 1 \\ \vdots & \ddots & \vdots & \ddots & \vdots & \vdots \\ \gamma_{m1} & \cdots & \gamma_{mi} & \cdots & \gamma_{mm} & 1 \\ 1 & \cdots & 1 & \cdots & 1 & 0 \end{bmatrix} \begin{bmatrix} \lambda_1 \\ \vdots \\ \lambda_i \\ \vdots \\ \lambda_m \\ \mu \end{bmatrix} = \begin{bmatrix} \gamma_{10} \\ \vdots \\ \gamma_{i0} \\ \vdots \\ \gamma_{m0} \\ 1 \end{bmatrix} \quad (12a)$$

Or equivalently,

$$\Gamma \times \Lambda = \Gamma_0 \quad (12b)$$

The ordinary kriging estimate  $\hat{z}(x_0)$  is calculated by substituting  $\lambda_i$  values into Equation (7). Variance of the estimation error, also known as the *ordinary kriging variance*, is

$$\sigma_{\text{ok}}^2(x_0) = E\{[Z(x_0) - \hat{Z}(x_0)]^2\} = \mu + \sum_{i=1}^m \lambda_i \gamma_{i0} \quad (13)$$

Readers are referred to Journal and Huijbregts (1978) for theoretical development of the ordinary kriging estimation method.

The following remarks can be made about the ordinary kriging system.

1. The  $\Gamma$  matrix in Equation (12b) is solely determined by measurement locations and the variogram  $\gamma(h)$ . Therefore, it reflects the effect of geometric configuration of the measurement locations on the ordinary kriging estimates.
2. The column vector  $\Gamma_0$  on the right-hand-side of equation(12b) depends on the distances between measurement locations  $x_i$ ,  $i = 1, 2, \dots, m$ , and the interpolation point  $x_0$ . It describes the spatial correlation between random variables  $Z(x_i)$  and  $Z(x_0)$ .
3. Given the semi-variogram  $\gamma(h)$ , the ordinary kriging variance  $\sigma_{\text{ok}}^2$  can be calculated without any measurements of  $Z(x_i)$  as the ordinary kriging weights  $\lambda_i$  and the Lagrange multiplier  $\mu$  depend entirely on the geometric configuration of  $x_i$  and  $x_0$ .
4. The ordinary kriging is an exact interpolator (de Marsily, 1986). If spatial estimation is to be made at a measurement location  $x_k$ ,  $x_k \in \{x_1, x_2, \dots, x_m\}$ , the ordinary kriging system yields  $\hat{z}(x_k) = z_k$ . It implies that  $\lambda_k = 1$ ,  $\lambda_i = 0$ ,  $i \neq k$ , and  $\text{Var}[\hat{Z}(x_k) - Z(x_k)] = 0$ .

## STUDY AREA AND DATA SET

Previous research (Hsu *et al.*, 1993) calculated total rainfall depths of 48 design storms (combinations of eight durations  $tr = 1, 2, 3, 4, 6, 12, 18$  and  $24$  h and six recurrence intervals  $T = 5, 10, 25, 50, 100$  and  $200$  years)

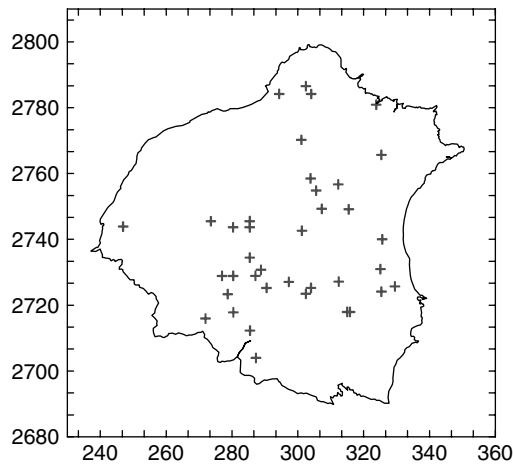


Figure 3. Rain-gauge locations ( $X$  and  $Y$  coordinates are Transverse Mercator projection in kilometres)

using rainfall data collected by a network of 38 rain gauges in northern Taiwan (see Figure 3). Elevations of rain-gauge sites vary from 5 m to 2000 m above mean sea-level. All stations have over 30 years of rainfall records. Design storm depths are calculated through hydrological frequency analysis:

1. collecting rainfall data of annual maximum series for selected design durations  $tr$ ;
2. fitting a probability distribution to the data of an annual maximum series and applying a test of goodness-of-fit such as the chi-squared test or the Kolmogorov–Smirnov test;
3. using the frequency factor equation (Chow *et al.*, 1988) to calculate total rainfall depths of the 48 design storms.

Hsu *et al.* (1993) applied the Kolmogorov–Smirnov test to annual maximum series for several types of distribution including log-normal, Pearson type III, log-Pearson type III and extreme value type I. The log-Pearson type III distribution was chosen for distribution fitting of various annual maximum rainfall series for all gauges. Design storm depths of the 38 rain-gauge sites are then considered as *measurements* of the 48 design storm random fields, and are used to interpolate design storm depths of ungauged locations.

#### DEVELOPING CONTOURS OF DESIGN STORM DEPTHS

Ordinary kriging estimation can be made for any point  $x_0$  in the spatial domain  $\Omega$  by solving the ordinary kriging system of Equation (12a). In order to develop rainfall depth contours of various design storms, we first discretize the study area by imposing a grid network with a 2-km grid interval.

Design storm depths at the 38 rain-gauge sites were used to calculate the *experimental semi-variogram* from

$$\hat{\gamma}(h) = \frac{1}{2|N(h)|} \sum_{N(h)} [z(x_i) - z(x_j)]^2, \quad h > 0 \tag{14}$$

where  $N(h) \equiv \{(x_i, x_j) : |x_i - x_j| = h; i, j = 1, 2, \dots, m\}$ . As semi-variograms must be conditionally negative definite, theoretical models are used to fit the *experimental semi-variogram*. Table I presents some of the commonly used semi-variogram models.

In this study the exponential model was chosen to fit the experimental semi-variograms of rainfall depths of the 48 design storms. Figure 4 demonstrates the fitted semi-variograms for rainfall depth of the (1 h, 5 year) and (24 h, 100 year) design storms. Given locations of the 38 rain-gauges and the variogram  $\gamma(h)$ , design storm

Table I. Commonly used semi-variogram models

Model type	Formula	Influence range	Sill
Exponential model	$\gamma(h) = \omega[1 - \exp(-h/a)]$	$3a$	$\omega$
Spherical model	$\gamma(h) = \begin{cases} \omega \left[ \frac{3}{2}(h/a) - \frac{1}{2}(h/a)^3 \right], & h \leq a \\ \omega, & h > a \end{cases}$	$a$	$\omega$
Gaussian model	$\gamma(h) = \omega[1 - \exp[-(h/a)^2]]$	$\sqrt{3}a$	$\omega$
Power model	$\gamma(h) = \omega h^\alpha, \alpha < 2$	$+\infty$	N/A

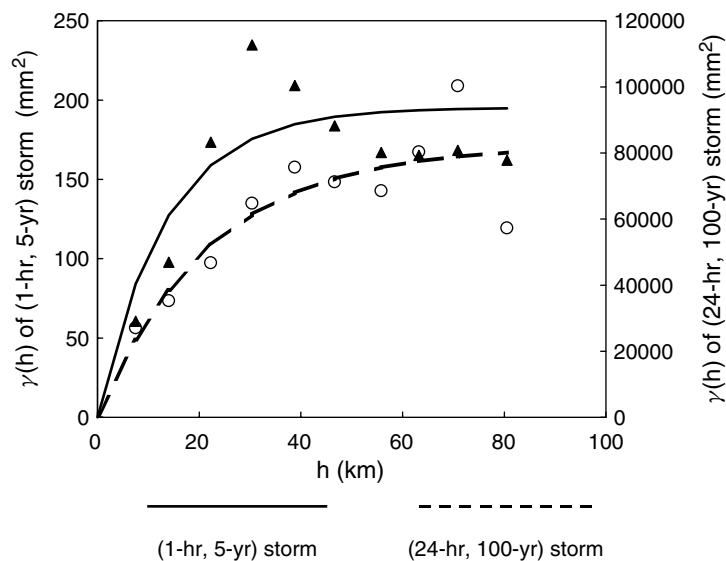


Figure 4. Experimental and fitted variograms for (1-hr, 5-yr) and (24-hr, 100-yr) design storm depths (dots marked by ▲ and ○ respectively represent experimental variograms of (1 h, 5-year) and (24 h, 100 year) design storm depths)

depths at any grid node  $x_0$  are interpolated by solving kriging weights  $\lambda_i$  in Equation (12a) and substituting them into Equation (7). Rainfall depth contours of various design storms were then established using design storm depths estimated at 2100 grid nodes. Examples of design storm depth contours and corresponding kriging variance contours are shown in Figure 5.

## DISCUSSION

As design storms are hypothetical events with respect to various combinations of duration and recurrence interval, rainfall depth measurements of these events do not exist. In order to validate the applicability of design storm contours established by ordinary kriging, we adopt three indirect ways to demonstrate that these design storm contours reveal important characteristics that are normally observed in natural storm events. Validation of design storm contours is made by consideration of: (i) significant contribution to annual rainfall by long-duration annual maximum rainfall depth, (ii) the spatial variation structure of individual design storms and (iii) the influence zone of each rain-gauge station.

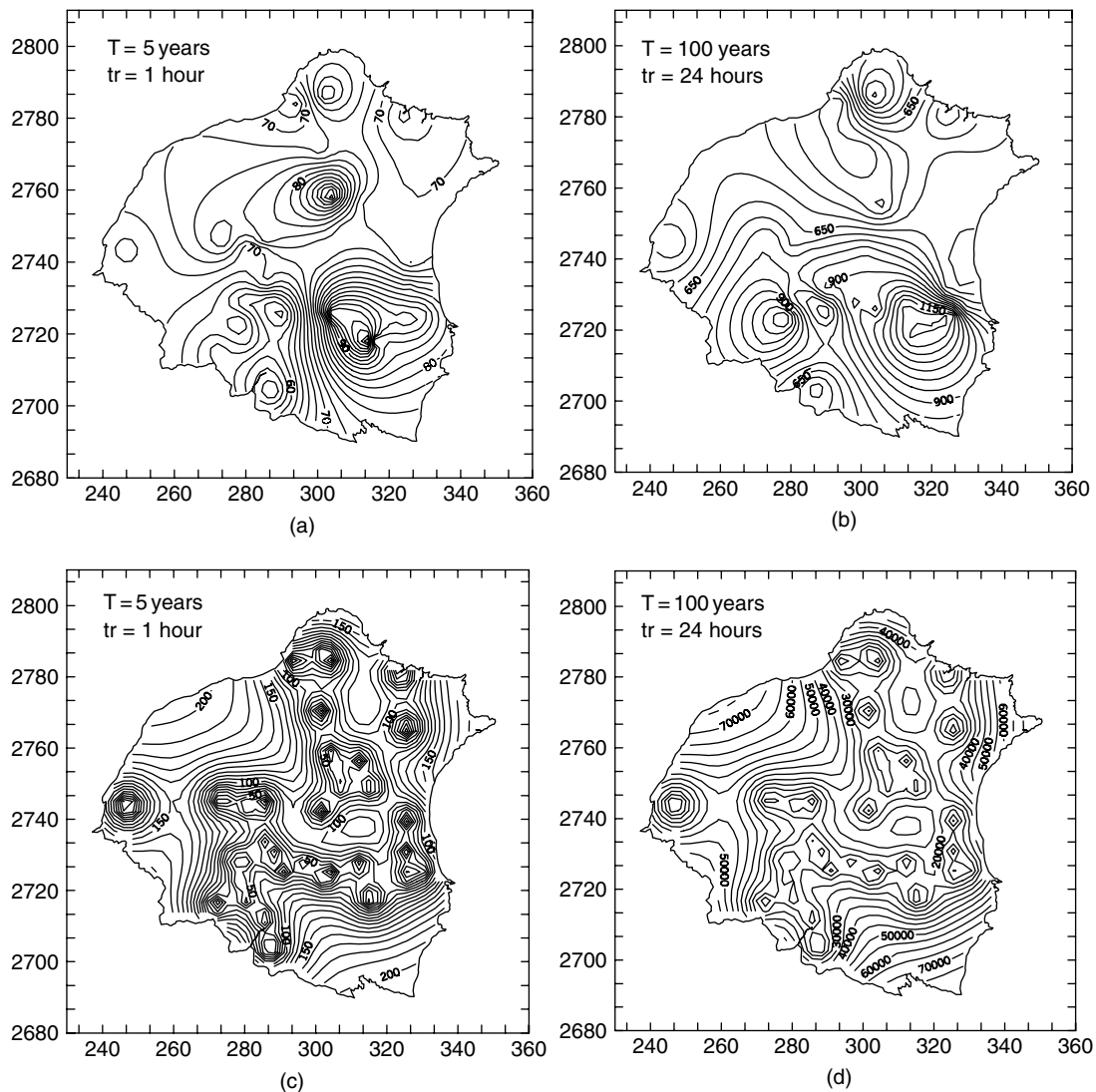


Figure 5. Examples of design storm contours (a, b) and their corresponding kriging variance contours (c,d). (Units are mm and mm<sup>2</sup> for contours in (a,b) and (c,d), respectively (X and Y coordinates are Transverse Mercator projection in kilometres)

*Comparison with the annual rainfall contours*

Design storm depths are derived from annual maximum rainfall depths of various *design durations* by means of hydrological frequency analysis. Here we emphasize that design durations are artificially designated durations used to determine the corresponding annual maximum rainfall depths, and in general do not coincide with the *actual* durations (referred to as *event durations*) of real storms. Cheng *et al.* (2001) found that a single severe storm event often produces annual maximum rainfalls of several design durations. Such storm events are referred to as the *annual maximum events*. Significant portions of the annual rainfall depths are contributed by annual maximum events; therefore, the pattern of annual rainfall contours is heavily dependent on the spatial variation of the rainfall depths produced by annual maximum events. Consequently, the average annual rainfalls and the design storm depths, particularly design storms of long duration and large recurrence

interval, are expected to have similar contour patterns. Figure 6 illustrates contour maps of the average annual rainfall depth and the 24 h, 200-year design storm depth for northern Taiwan. Four heavy rainfall centres, marked A, B, C and D, of the average annual rainfalls correspond perfectly to the design storm centres A', B', C' and D', respectively. For sites A and B, the 24 h, 200-year design storm depths account for approximately one-sixth of the average annual rainfalls. For sites C and D, the 24 h, 200-year design storm depth accounts for approximately one-quarter and one-half of the average annual rainfall, respectively. The similarity between spatial variations of the average annual rainfall and the 24 h, 200-year design storm depth is a strong indication of practical usage for the contour maps of long duration and large recurrence interval design storms.

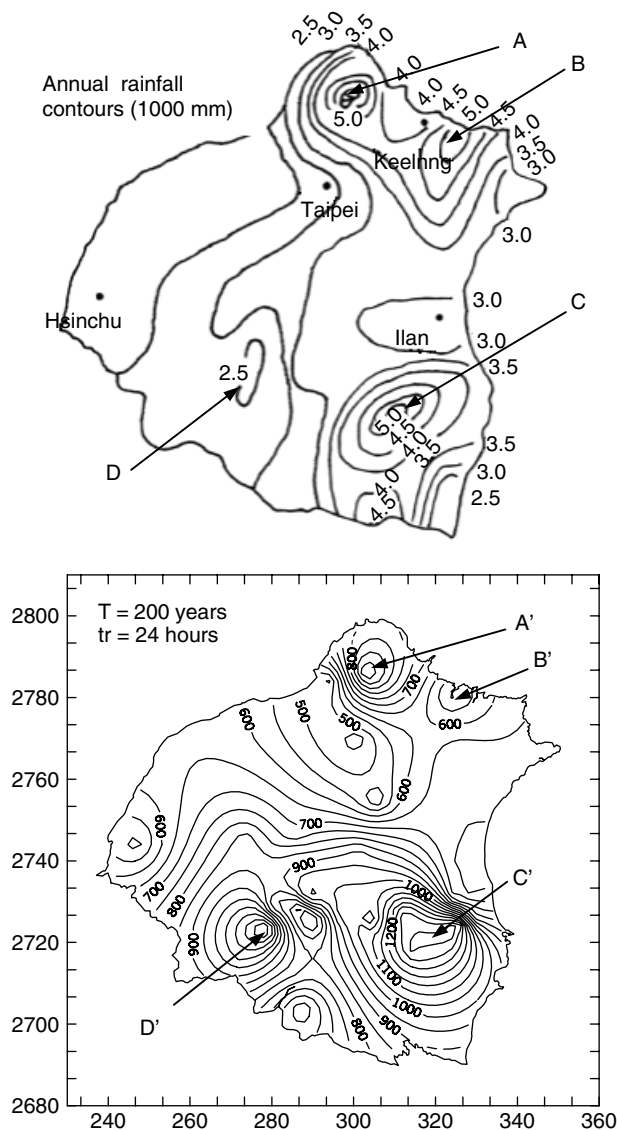


Figure 6. Contour maps of average annual rainfall and the 24 h, 200-year design storm depth (X and Y coordinates are Transverse Mercator projection in kilometres)

*Comparison with the index-rainfall method*

Hsu *et al.* (1993) studied the rainfall depths of various design storms in Taiwan and developed an approach for interpolation of the design storm depth based on average annual rainfall. The approach establishes empirical relationships for the average annual rainfall and design storm depths, and uses contours of the average annual rainfall to aid the interpolation of design storm depths. The approach is briefly described below.

Let  $I_t^T$  represent the rainfall intensity (in mm/h) of a design storm of duration  $t$  (in minutes) and recurrence interval  $T$  (in years). Also let  $P$  denote the average annual rainfall depth (in millimetres). The 60 min, 25-year design storm depth,  $I_{60}^{25}$ , is used as an index-storm to associate rainfall depths of various design storms through the following equation

$$\frac{I_t^T}{I_{60}^{25}} = (G + H \log_{10} T) \frac{A}{(t + 55)^C} \tag{15}$$

Constants  $A$ ,  $C$ ,  $G$  and  $H$ , and the index storm depth  $I_{60}^{25}$  are site-specific. The index-storm concept was firstly proposed by Bell (1969) to establish generalized intensity-duration-frequency (IDF) relationships in Australia. Chen (1983) also developed similar relationships for design storm depths in the USA.

The following empirical formulae were further established to determine site-specific constants  $A$ ,  $C$ ,  $G$  and  $H$ , and the index storm depth  $I_{60}^{25}$  using only the average annual rainfall  $P$

$$A = \left( \frac{P}{-189.96 + 0.31P} \right)^2 \tag{16}$$

$$C = \left( \frac{P}{-381.71 + 1.45P} \right)^2 \tag{17}$$

$$G = \left( \frac{P}{42.89 + 1.33P} \right)^2 \tag{18}$$

$$H = \left( \frac{P}{-65.33 + 1.84P} \right)^2 \tag{19}$$

$$I_{60}^{25} = \left( \frac{P}{25.29 + 0.094P} \right)^2 \tag{20}$$

Finally, rainfall depths of design storms at any location can be estimated by using Equations (15)–(20) and an average-annual-rainfall contour map. We shall refer to this approach as the index-rainfall method. The index-rainfall method is based on the perception that average annual rainfalls are available at many rain-gauge sites and they exhibit less spatial variation, therefore, a contour map of the average annual rainfall is more reliable and Equations (15)–(20) will yield accurate estimates of design storm depths.

Estimates at four rain-gauge sites, Taipei, Keelung, Hsinchu and Ilan (see Figure 6), are used to compare the interpolation accuracy of the index-rainfall method and the ordinary kriging method. Table II illustrates examples of the design storm depths calculated by the frequency analysis (which are considered as *measurements*) and their estimates by the index-rainfall and ordinary kriging methods. The ordinary kriging is an exact interpolator, i.e. theoretically it yields zero estimation errors at measurement locations. In Table II, discrepancies between design storm depths calculated by frequency analysis (the IDF curves) and by ordinary kriging method exist because the ordinary kriging estimates are values *read* from contour maps (e.g. Figure 5). Figure 7 clearly demonstrates that ordinary kriging is superior to the index-rainfall method in terms of the interpolation accuracy.

The index-rainfall method has the advantage of simplicity as it requires only the average annual rainfall depth to estimate rainfall depths of any design storms. It also implies two features:

Table II. Examples of design storm depths (mm) calculated by frequency analysis and their estimates by ordinary kriging (OK) and index-rainfall method

<i>tr</i> (h)	Taipei (2126 mm <sup>a</sup> )						Keelung (3208 mm <sup>a</sup> )					
	IDF		OK		Index-rainfall		IDF		OK		Index-rainfall	
	<i>T</i> = 5	<i>T</i> = 100	<i>T</i> = 5	<i>T</i> = 100	<i>T</i> = 5	<i>T</i> = 100	<i>T</i> = 5	<i>T</i> = 100	<i>T</i> = 5	<i>T</i> = 100	<i>T</i> = 5	<i>T</i> = 100
6	157.4	258.7	160	260	200	305	161.3	258.4	160	280	234	355
12	197.4	320.8	200	320	272	414	221.6	352.5	240	375	329	499
24	242.4	393.9	260	410	362	551	283.6	448.1	300	500	455	689

<i>tr</i> (h)	Hsinchu (1749 mm <sup>a</sup> )						Ilan (2688 mm <sup>a</sup> )					
	IDF		OK		Index-rainfall		IDF		OK		Index-rainfall	
	<i>T</i> = 5	<i>T</i> = 100	<i>T</i> = 5	<i>T</i> = 100	<i>T</i> = 5	<i>T</i> = 100	<i>T</i> = 5	<i>T</i> = 100	<i>T</i> = 5	<i>T</i> = 100	<i>T</i> = 5	<i>T</i> = 100
6	171.9	282.9	180	300	180	275	192.1	323.7	195	320	203	310
12	218.1	361.4	240	375	239	365	262.0	446.6	280	450	277	422
24	269.0	442.2	280	475	309	473	343.1	585.3	360	600	371	564

<sup>a</sup> Average annual rainfall.

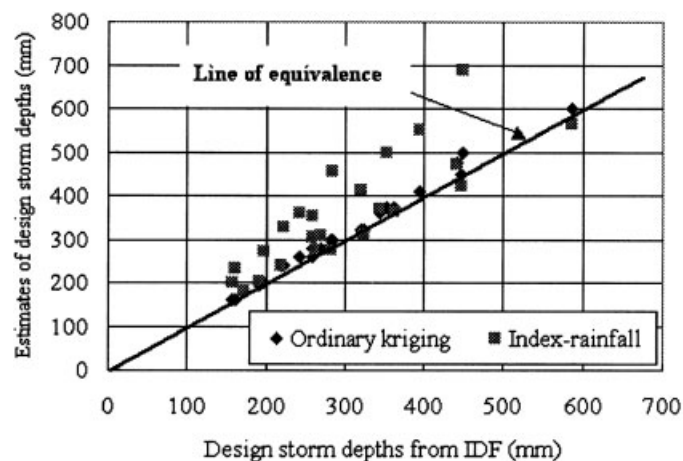


Figure 7. Design storm depths and their estimates by ordinary kriging and index-rainfall methods (see data in Table II)

1. all locations with the same average annual rainfalls have exactly the same design storm depths:
2. the index-rainfall method always yields higher design storm depths for locations with higher average annual rainfalls.

However, such relationships, in general, do not exist between the average annual rainfalls and the design storm depths calculated by frequency analysis. For example, Hsinchu has lower average annual rainfall (1749 mm) than Taipei (2126 mm), however, its 6 h, 5 year design storm depth is higher (171.9 mm versus 157.4 mm). In the next section we demonstrate that the average annual rainfall and the design storm depths may have significantly different spatial variation structures. The index-rainfall method fails to distinguish the spatial variations of the design storm depth and the average annual rainfall. On the contrary, the ordinary kriging method establishes the spatial variation structure for each individual design storm, and therefore circumvents the above erroneous situation.

### *Spatial variation characteristics of design storms*

As introduced previously, parameters of the semi-variogram represent certain spatial variation characteristics of the random field. In this section we examine values of the variogram parameters and their implications for the spatial variation characteristics of design storms. We first make three remarks about the random characteristics of design storms:

1. the design storms, by definition, characterize the characteristics of extreme events;
2. the degree of extremity increases with the increase of recurrence interval and decrease of design storm duration;
3. the degree of spatial independence increases (or the spatial correlation decreases), as the extremity of the storm event increases.

Figure 8 illustrates that variogram parameters, the practical influence range ( $3a$ ) and sill ( $\omega$ ), are functions of the recurrence interval and the design storm duration. Their relationships are well consistent with the random characteristics of design storms.

The sill  $\omega$  represents the variance of the random field under investigation, i.e. the total rainfall depth of the design storm in this study. Storm events of various seasons and intensities have different spatial variation structures; therefore, it would be unrealistic to adopt a unique variogram for all storm events irrespective of the season, meteorological conditions and rainfall intensity. Bastin *et al.* (1984) adopted a *climatological variogram* model of the form

$$\gamma(m, h) = \alpha(m)\gamma^*(h) \quad (21)$$

where  $m$  is an index for storm events,  $h$  is the Euclidian distance and  $\alpha(m)$  is the scaling factor. With this structure, all the time non-stationarity is concentrated in the scale factor  $\alpha(m)$ , whereas the component  $\gamma^*(h)$  is time invariant and is called the *scaled climatological variogram*. Lebel *et al.* (1987) pointed out that in a region of relatively regular weather patterns, the scaling factor  $\alpha(m)$  mainly reflects the seasonal variation of the spatial structure of the rainfall field. For example, in Taiwan annual maximum rainfall depths are mostly produced by two dominant storm types: mesoscale thunderstorms and synoptic scale tropical cyclones, during the period between May and November. Therefore, if the climate pattern persists,  $\alpha(m)$  accounts for the difference in spatial structure of storm types. In regions where the climatic variability is stronger, the factor  $\alpha(m)$  mainly accounts for the scale effect as a result of the variation in time of the mean rainfall intensity.

The scale factor in Equation (21) is equivalent to the sill  $\omega$ , or the variance of the rainfall field; therefore, design storms with higher total rainfall depths will have higher sill values, as depicted in Figure 8.

For design storms with duration  $tr$  smaller than 6 h, the increase in the recurrence interval or decrease in the storm duration corresponds to decreases in the influence range and spatial correlation of design storm depth. For example, rainfall depths of the 1 h, 200-year design storm are highly independent in space, and the semi-variogram shows a near pure nugget effect. However, for design storms with design durations greater than or equal to 6 h, the influence ranges do not vary significantly, with an average of approximately 72 km ( $a \approx 24$  km). In Taiwan, short-duration storms ( $tr < 6$  h) are mostly convective cells or thunderstorms, whereas long-duration storms are mostly tropical storms or cyclones. Eagleson (1970) pointed out that tropical storms often have a common substructure consisting of more or less parallel mesoscale events, regardless of their synoptic scales. The nearly constant influence range of long-duration storms represents a unique characteristic of tropical storms in the study area. Whether it is related to the characteristic dimension of mesoscale events in tropical storms requires further investigation.

As seen in Figure 8, some design storms with short durations and long recurrence intervals have very small influence ranges. Rainfall depths of such design storms have high spatial variations and their influence ranges are smaller than most of the interstation distances. Spatial interpolation/estimation of such design storms may encounter difficulties as described below.

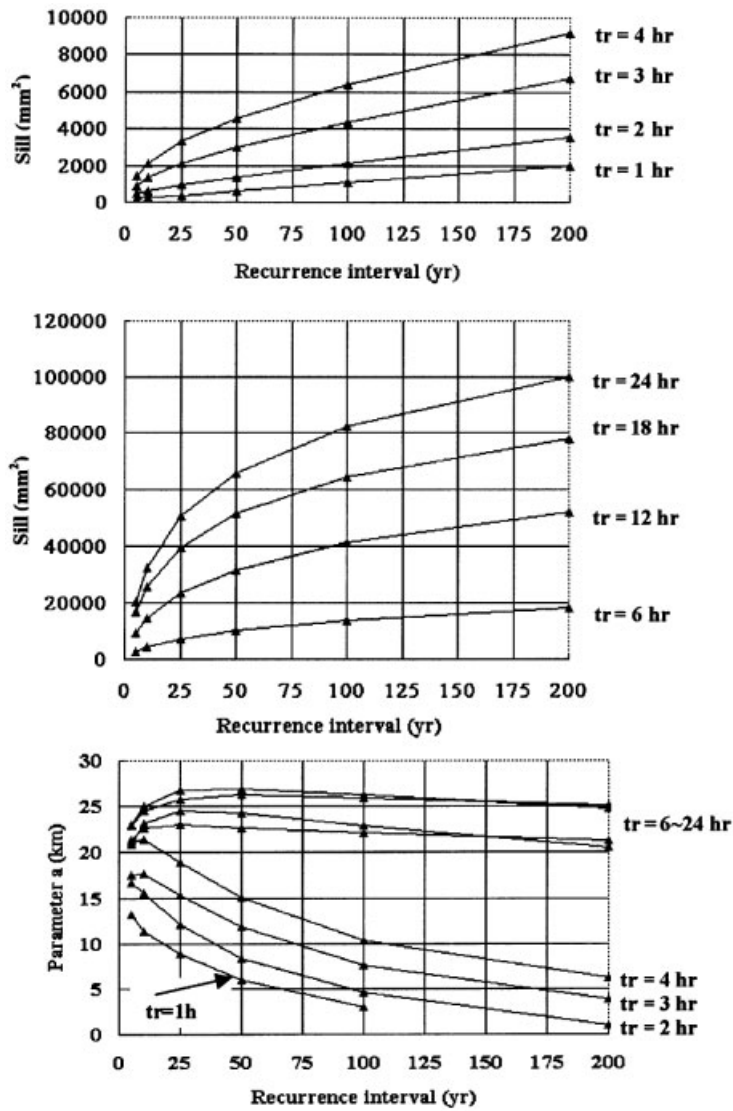


Figure 8. Variogram parameters for rainfall depth of various design storms

Consider the situation that the influence range of rainfall depth is smaller than any interstation distances and distances between rain-gauge locations and the interpolation point. As the variogram  $\gamma(h)$  reaches its sill when  $h$  exceeds the influence range, then, values of  $\gamma_{ij}$ , ( $i \neq j$ ) and  $\gamma_{i0}$  ( $i, j = 1, 2, \dots, m$ ) in Equation (12a) all equal the constant sill  $\omega$ . As a result, all rain-gauge sites have equal weights and

$$\lambda_1 = \lambda_2 = \dots \lambda_m = \frac{1}{m} \tag{22}$$

and

$$\mu = \frac{\omega}{m} \tag{23}$$

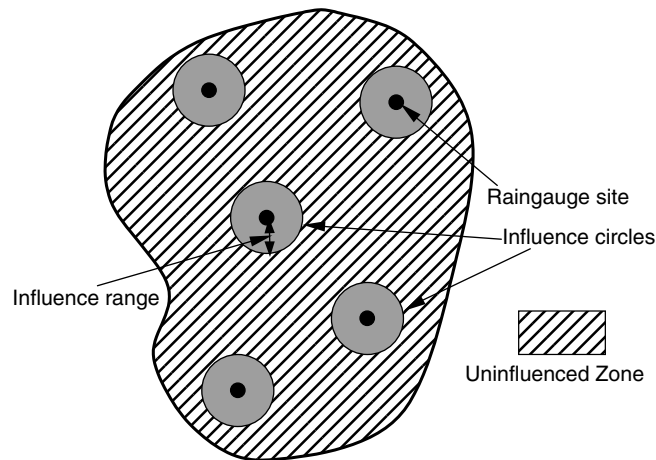


Figure 9. Influence circles and the uninfluenced zone

Therefore, the interpolated rainfall depth and its kriging variance are respectively

$$\hat{z}(x_0) = \frac{1}{m} \sum_{i=1}^m z(x_i) \quad (24)$$

$$\sigma_{\text{ok}}^2(x_0) = \left(1 + \frac{1}{m}\right) \omega \quad (25)$$

Figure 9 illustrates that if the influence range of rainfall depth is smaller than any interstation distances, then ungauged locations not within the *influence circle* of any rain gauge will have exactly the same rainfall estimates and kriging variances, respectively determined by Equations (24) and (25). The areal extent of such locations is referred to as the *uninfluenced zone*. As the influence range becomes smaller, the uninfluenced zone expands and occupies a vast region of the study area. Figure 10 demonstrates rainfall contour maps of a 1 h, 100-year design storm established by the ordinary kriging method and the traditional inverse-distance-weighting method. The rainfall contour map of the ordinary kriging method shows isolated contours in the neighbourhood of the rain-gauge locations and no contours in the uninfluenced zone. The inverse-distance-weighting method yields smoother contours and is not adequate for contouring rainfall depths of design storms with high spatial variations. This result demonstrates the advantage of using ordinary kriging over the traditional inverse-distance-weighting method that does not consider the influence range of the rainfall field and always yields contours even in the uninfluenced zone. In this study, rainfall depth contours developed by the ordinary kriging method for design storms of ( $tr = 1$  h,  $T = 100$  year) ( $tr = 2$  h,  $T = 100$  year), ( $tr = 1$  h,  $T = 200$  year), ( $tr = 2$  h,  $T = 200$  year), and ( $tr = 3$  h,  $T = 200$  year) were not recommended for practical usage.

Ordinary kriging not only yields rainfall estimates at ungauged locations, it also calculates the variance of the estimation error, or the *ordinary kriging variance*, for every estimate using Equation (13). The contours of kriging variance (see Figure 5) provide information for comparison of site-specific estimation accuracies.

## CONCLUSIONS

In this study we consider the spatial distribution of the design storm depth as a random field and show that the spatial variation structure of the design storm depth varies with duration and recurrence interval of the

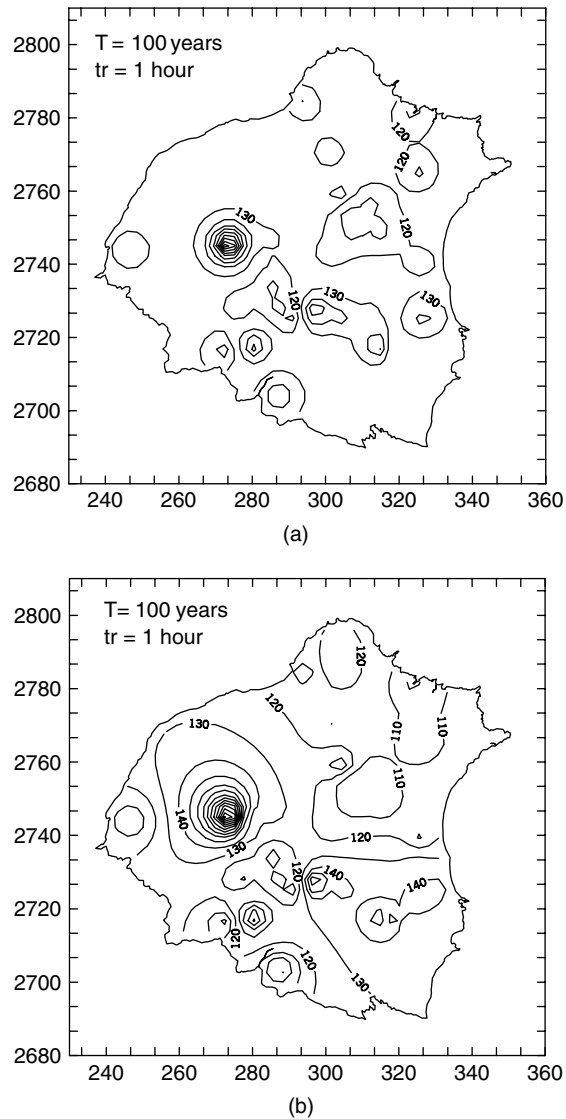


Figure 10. Rainfall contour maps of 1 h, 100-year design storm depths (in millimetres) established by the ordinary kriging method (a) and the inverse-distance-weighting method (b) (X and Y coordinates are Transverse Mercator projection in kilometres)

design storm. By adopting three indirect ways, we demonstrate that design storm contours established by the ordinary kriging method reveal important characteristics that are normally observed in natural storm events.

We also demonstrate that the spatial variation structures of the average annual rainfall and the design storm depths may be significantly different and the index-rainfall method fails to distinguish this difference. On the contrary, the ordinary kriging method establishes spatial variation structure for each individual design storm, and therefore yields better rainfall estimates.

Variogram parameters, the sill and practical influence range, are functions of the recurrence interval and the storm duration. The sill accounts for the time non-stationarity of the rainfall field, and design storms with higher total rainfall depths have higher sill values. Variation in the sill value may arise from variation of dominant storm types and changes in rainfall intensity owing to climate change. Effect of climate change on

the spatial variation characteristics of design storms requires further study. In this regard, a continuous storm rainfall simulation model capable of simulating the occurrence of storm events of various storm types and the time distribution of storm rainfall depth based on given climate change scenarios will be of great value.

For design storms with duration smaller than 6 h, the increase in the recurrence interval or decrease in the storm duration corresponds to decreases in the spatial correlation. However, for design storms with design durations greater than or equal to 6 h, the influence ranges do not vary significantly, with an average of approximately 72 km. The nearly constant influence range of long-duration storms represents a unique characteristic of tropical storms in the study area. Some design storms with short durations and long recurrence intervals have high spatial variations and their influence ranges are smaller than most of the interstation distances. Rainfall contour maps of such design storms usually have dense contours in the neighbourhood of rain-gauge sites and no contours in the uninfluenced zone, which may occupy a vast region of the study area. Such contour maps should not be recommended for practical usage.

#### ACKNOWLEDGEMENTS

We acknowledge the financial support of the National Science Council (NSC-87-2313- B-002-048) and the Water Resources Agency, Ministry of Economic Affairs of Taiwan, ROC. We also thank the anonymous reviewers for their constructive comments and suggestions that were very helpful in revising the manuscript.

#### REFERENCES

- Bastin G, Lorent B, Duque C, Gevers M. 1984. Optimal estimation of the average areal rainfall and optimal selection of raingauge locations. *Water Resources Research* **20**(4): 463–470.
- Bell FC. 1969. Generalized rainfall–duration–frequency relationships. *Journal of the Hydraulics Division, Proceedings of the American Society of Civil Engineers* **95**(HY1): 311–327.
- Chang TK, Shyu GS, Lin YP, Chang NC. 1999. Geostatistical Analysis of Soil Arsenic Content in Taiwan. *Journal of Environmental Science and Health, Part A* **34**(7): 1485–1501.
- Chen CL. 1983. Rainfall intensity–duration–frequency formulas. *Journal of Hydraulic Engineering* **109**(12): 1603–1621.
- Cheng KS, Hueter I, Hsu EC, Yeh HC. 2001. A scale-invariant Gauss–Markov model for design storm hyetographs. *Journal of the American Water Resources Association* **37**(3): 723–736.
- Chow VT, Maidment DR, Mays LW. 1988. *Applied Hydrology*. McGraw-Hill: New York, NY; 572 pp.
- De Marsily G. 1986. *Quantitative Hydrogeology*. Academic Press: Orlando; 440 pp.
- Eagleson PS. 1970. *Dynamic Hydrology*. McGraw-Hill: New York, NY; 462 pp.
- Hershfield DM. 1961. *Rainfall Frequency Atlas of the United States*. Technical Paper No. 40, U.S. Department of Commerce, Weather Bureau: Washington, DC.
- Hsu MH, Cheng KS, Yih VJ, Lin GF, Wu PL. 1993. *Design Storm Analysis in Taiwan*. Hydraulic Research Laboratory, National Taiwan University. (In Chinese).
- Hughes JP, Lettenmaier DP. 1981. Data requirements for kriging: estimation and network design. *Water Resources Research* **17**(6): 1641–1650.
- Journel AG, Huijbregts CJ. 1978. *Mining Geostatistics*. Academic Press: London; 600 pp.
- Lebel T, Bastin G, Obled C, Creutin JD. 1987. On the accuracy of areal rainfall estimation: a case study. *Water Resources Research* **23**(11): 2123–2134.
- Rao DV. 1991. *24-hour Rainfall Distributions for Surface Water Basins within the St. Johns River Water Management District*. Technical Publication SJ91-3, St. Johns River Water Management District: Palatka, Florida; 60 pp.
- Viessman W Jr, Lewis GL, Knapp JW. 1989. *Introduction to Hydrology*. Harper and Row: New York, NY; 780 pp.
- Wackernagel H. 1995. *Multivariate Geostatistics*. Springer-Verlag: Berlin; 256 pp.